Top Curr Chem (2015)
DOI: 10.1007/128_2015_630

Ensemble DFT Approach to Excited States of Strongly Correlated Molecular Systems

Michael Filatov

Abstract Ensemble density functional theory (DFT) is a novel *time-independent* formalism for obtaining excitation energies of many-body fermionic systems. A considerable advantage of ensemble DFT over the more common Kohn–Sham (KS) DFT and time-dependent DFT formalisms is that it enables one to account for strong non-dynamic electron correlation in the ground and excited states of molecular systems in a transparent and accurate fashion. Despite its positive aspects, ensemble DFT has not so far found its way into the repertoire of methods of modern computational chemistry, probably because of the perceived lack of practically affordable implementations of the theory. The spin-restricted ensemble-referenced KS (REKS) method is perhaps the first computationally feasible implementation of the ideas behind ensemble DFT which enables one to describe accurately electronic transitions in a wide class of molecular systems, including strongly correlated molecules (biradicals, molecules undergoing bond breaking/formation), extended π-conjugated systems, donor–acceptor charge transfer adducts, etc.

Keywords Charge transfer excitation energies · Ensemble density functional theory · Excited electronic states · Non-dynamic electron correlation

Contents

M. Filatov (✉)
Institut für Physikalische und Theoretische Chemie, Universität Bonn, Beringstr. 4, 53115 Bonn, Germany
e-mail: mike.filatov@gmail.com

1 Introduction

The founding principles of density functional theory (DFT) were initially formulated only for the ground states of fermionic many-body systems [1, 2]. It is therefore commonly accepted that the excited states in the context of DFT can be accessed by the use of some form of response formalism implemented, for instance, in the time-dependent DFT (TD-DFT) methods [3, 4]. In principle, TD-DFT is a rigorous formulation of the ground state DFT for time-dependent phenomena [5]. However the excitation energies of many-body systems are typically accessed with the use of the linear response (LR) formalism, which assumes that the time dependence stems from a weak (usually oscillatory) perturbing potential [3–5]. In practice, LR-TD-DFT yields a very reasonable description of optical absorption spectra with the use of the commonly available ground-state approximate density functionals [3, 4]; however, some spectacular failures of the formalism are also known. In particular, standard implementation of LR-TD-DFT relies on the adiabatic approximation (i.e., locality of the exchange-correlation (XC) kernel in the time domain) and consequently cannot take proper account of multiple excitations [6, 7], which become important, e.g., for excited states of conjugated molecular systems [8]. Yet another failure of the standard LR-TD-DFT to describe the excited states of strongly correlated systems, e.g., H_2 at stretched bondlength [9], can be traced back to the use of the standard ground-state Kohn–Sham (KS) formalism [2] which fails to take proper account of the non-dynamic electron correlation.

In the domain of wavefunction theory (WFT), the excited states of molecules can be obtained from the ground-state response formalism as well as the variational excited state formalism [10]. An appealing idea is to employ the (time-independent) variational formalism to obtaining excitation energies in the context of DFT. Indeed, the first attempts to calculate the excitation energies by taking the energy differences between the variationally obtained ground state energy and the energy of a state obtained by promoting an electron to unoccupied energy level, the so-called ΔSCF approach,[1] date back to the early 1970s [11, 12]. However, despite some attempts to justify the ΔSCF approach for computing the energies of one-electron transitions between the states of different spatial symmetry [13, 14], the idea of variationally obtaining the energy of an individual excited state in the context of DFT lacks firm theoretical background [15–17].

A rigorous way of developing time-independent formalism for obtaining excitation energies in the context of DFT is offered by *ensemble* DFT [18, 19] which

[1] For more details on ΔSCF, see the chapter "A Constricted Variational Density Functional Theory Approach to the Description of Excited States" by T. Ziegler, M. Krykunov, I. Seidu, and Y. C. Park.

operates with weighted sums (ensembles) of fractionally occupied (ground and excited) states. The ensemble representation of the density and the energy for an arbitrary many-body fermionic system was put on a firm theoretical ground by Lieb [20] and Englisch and Englisch [21, 22], and was later extended to the domain of excited states by Gross et al. [23–25].

A practical demonstration of the necessity to invoke the ensemble representation for mapping the density of a strongly correlated system onto a non-interacting KS reference was achieved by Baerends et al. [26, 27] in first-principles numeric simulations employing the (nearly) exact molecular densities, which was later confirmed by Morrison [28] in a series of first-principles atomic calculations. Although the ensemble formalism enables one to obtain excitation energies in a rigorous and computationally convenient way [5], the progress in this direction was extremely slow [29–33], perhaps because of the perceived lack of suitable density functionals capable to accommodate the densities with fractional occupation numbers (FONs).

A practically accessible approach to the calculation of the strongly correlated ground and excited states of molecules which employs the ideas behind ensemble DFT was achieved in the form of the spin-restricted ensemble-referenced KS (REKS) method [34–41]. The method was initially developed for the ground states of strongly correlated molecular systems [34–38] and was later extended to the domain of excited state calculations [39–41]. Although the REKS method is founded on a rigorous theoretical background [20, 21, 26] and was successfully applied to study situations often intractable with the use of the conventional KS DFT methods [37, 38, 40–61], the method has received a little attention in the literature and has been largely overlooked by the computational chemistry community. In this chapter, an overview of the REKS methodology and its connection to the ensemble DFT formalism is given with emphasis on the use of the method to obtain excited states of molecular systems.

2 Ensemble DFT

The basic tenet of KS DFT is that any physical fermionic ground state density $\rho(\mathbf{r})$ can be uniquely mapped onto the ground state density $\rho_s(\mathbf{r})$ of a fictitious system of non-interacting particles moving in a suitably modified external potential $v_s(\mathbf{r})$. If such a $v_s(\mathbf{r})$, which is also known as the KS potential, can be found, the respective KS Hamiltonian $\hat{H}_s$ is minimized by a single Slater determinant (KS determinant) constructed from the lowest-energy one-electron functions (KS orbitals) $\varphi_{s,i}(\boldsymbol{r})$ and the non-interacting density $\rho_s(\boldsymbol{r})$ is

$$\rho_s(\mathbf{r}) = \sum_i 2\left|\varphi_{s,i}(\mathbf{r})\right|^2; \quad \forall \varepsilon_i \leq \mu\,, \tag{1}$$

where ε_i are the respective eigenvalues, μ is the Fermi level, and a closed electronic

shell is assumed [1, 2]. The physical density $\rho(\mathbf{r})$ which can be mapped onto such a non-interacting density $\rho_s(\mathbf{r})$ is said to be non-interacting pure state v-representable, or PS-VR for brevity [21]. Naturally, in the case of non-interacting particles, such a pure state wavefunction is represented by a single KS determinant and one may speak of a determinantal v-representability (D-VR) as well [21].

A general proof of the existence of such a KS potential $v_s(\mathbf{r})$ and of the PS-VR property has never been achieved for an arbitrary physical density. By contrast, rigorous theoretical arguments have been given in favor of an alternative representation of an arbitrary fermionic density $\rho(\mathbf{r})$ by an ensemble (weighted sum) of a finite number (M) of the densities $\rho_K(\mathbf{r})$ originating from the same physical external potential $v_{\text{ext}}(\mathbf{r})$ [19–21]:

$$\rho(\mathbf{r}) = \sum_{K=1}^{M} \lambda_K \rho_K(\mathbf{r}), \quad \lambda_K \geq 0, \quad \sum_{K=1}^{M} \lambda_K = 1\,. \tag{2}$$

For the ensemble v-representable (E-VR) densities, the existence of a universal density functional $F[\rho]$ and its differentiability with respect to the density $\rho(\mathbf{r})$ were rigorously proved [20, 21], thus confirming the existence of the KS potential $v_s(\mathbf{r})$ and the respective non-interacting KS system.

Initially, ensemble DFT was formulated for ground state ensembles [20, 21], which implied that one could speak of averaging over degenerate electronic states. It is natural to assume that the degeneracy is imposed by the symmetry of the system. This seems a plausible assumption in the case of interacting particles, although for the non-interacting fermions (such as the KS reference system) there is a possibility of accidental degeneracy of several electronic configurations as was demonstrated in first principles numeric experiments by Schipper et al. [26] and by Morrison [28]. In these works it was shown that, when obtaining the KS potential $v_s(\mathbf{r})$ from the known (nearly) exact density [62], the fractional occupation numbers of several KS orbitals (i.e., the ensemble representation) have to be invoked. Thus, certain physical (i.e., interacting) PS-VR densities (the target densities were obtained from the accurate ab initio WFT calculations) can only be mapped onto the non-interacting E-VR densities. Remarkably, these target densities were obtained for molecular systems for which it was known that their electronic structure is dominated by the non-dynamic electron correlation; [63] in particular, the rectangular $H_2 + H_2$ system, the ground state of the C_2 molecule [26], and the ground state of a series of Be-like atomic ions [28] were investigated. For these atomic and molecular systems it is well established that, at the ab initio WFT level, their ground state wavefunctions require a multi-reference description, which is typically associated with the strong non-dynamic correlation [63].

The ensemble representation of the non-interacting KS reference system leads naturally to the fractional occupation numbers of KS orbitals:

$$\rho_s(\mathbf{r}) = \sum_i n_i \left|\varphi_{s,i}(\mathbf{r})\right|^2, \tag{3}$$

where the FONs satisfy the conditions

$$\begin{array}{cc} n_j = 2, & \varepsilon_j < \mu \\ 0 \le n_k \le 2, & \varepsilon_k = \mu \\ & \sum_i n_i = N \end{array}, \tag{4}$$

that is, only a few KS orbitals which degenerate at the Fermi level μ are allowed to have fractional occupations [26]. Alternatively, the ensemble density (*3*) can be written down as in (2) as a weighted sum of the densities $\rho_{s,K}$ (**r**) of several KS determinants constructed from a common set of KS orbitals; the ensemble weighting factors λ_K are then connected to the FONs in (*3*) via $\lambda_K = n_k/m$ where m is the number of electrons in the KS orbitals degenerate at the Fermi level and all the KS orbitals in the determinant yielding the $\rho_{s,K}$ (**r**) density are set doubly occupied. Recently, the degeneracy of the fractionally occupied KS orbitals at the Fermi level was rigorously proved [64].

For the ensemble density (2), Lieb proved [20] that the ground state energy is given by a weighted sum

$$E[\rho] = \sum_{K=1}^{M} \lambda_K E[\rho_K], \tag{5}$$

of the energies $E[\rho_K]$ of the ensemble components taken with the same weighting factors as in (2). Englisch and Englisch proved the differentiability of the ensemble energy $E[\rho]$ with respect to the ensemble density, thus demonstrating the existence of $v_s(\mathbf{r})$ and the ensemble KS reference system [21].

The energies of the non-interacting KS reference states constructed in [26] for the C_2 molecule and for the $H_2 + H_2$ system satisfy (5), provided that the ensemble densities are allowed. If, however, one insisted on having PS-VR (or D-VR) KS reference states for these molecular systems, holes below the Fermi level were observed which implied the breakdown of the basic assumption behind the KS method, namely that the density $\rho_s(\boldsymbol{r})$ is constructed from the *lowest* one-particle eigenstates of the non-interacting KS Hamiltonian. Besides that, the single determinant KS states found in [26] (and in [28]) had somewhat higher energies than the respective ensemble KS solutions. Thus, the ensemble KS solutions had to be preferred on the grounds of the variational principle. These conclusions have been fully confirmed by Morrison [28] in the study of Be isoelectronic series of atomic ions, for which mapping of the exact densities onto the KS reference could only be achieved with the use of ensemble densities, i.e., densities with the fractional occupation numbers of the valence 2s and 2p atomic orbitals. An attempt to formalize these observations and to develop ensemble variants of the KS theory

was undertaken in [30]; however this did not materialize in the form of a practically accessible computational scheme.

The ground-state ensemble DFT formalism was extended into the domain of excited state calculations in the works of Theophilou [18] and Gross et al. [23] who demonstrated that the Hohenberg–Kohn theorem is satisfied not only by the ground-state density and the energy but also by the density and the energy of an ensemble of several lowest energy states (i.e., the ground and excited states) of a many-body fermionic system. In particular, Gross et al. [23] proved that the ensemble energy (5) constructed from several lowest eigenstates of a many-body Hamiltonian $\hat{H}$ satisfies the variational principle

$$\sum_{K=1}^{M}\lambda_K\langle\Phi_K|\hat{H}|\Phi_K\rangle \geq \sum_{K=1}^{M}\lambda_K E_K; \quad 0 \leq \lambda_K \leq 1; \quad \sum_{K=1}^{M}\lambda_K = 1\,, \tag{6}$$

where Φ_k are the trial wavefunctions and E_K are the exact eigenvalues of the Hamiltonian $\hat{H}$ [23].

The variational character of the ensemble energy enables one to calculate excitation energies rigorously using (formally ground-state) density functionals. Considering only two state ensembles (the ground state E_0 and the lowest excited state E_1), for which the energy and the density are given by (7) and (8),

$$E_\omega = (1-\omega)E_0 + \omega E_1, \tag{7}$$

$$\rho_\omega(\mathbf{r}) = (1-\omega)\rho_0(\mathbf{r}) + \omega\rho_1(\mathbf{r}), \tag{8}$$

the excitation energy $\Delta E = E_1 – E_0$ can be obtained in two ways [5]. The first obtains ΔE for some fixed weighting factor ω, which trivially leads to

$$\Delta E = E_1 - E_0 = \frac{E_\omega - E_0}{\omega}, \tag{9}$$

and the second employs derivatives of E_ω with respect to the weighting factor [5, 29]

$$\Delta E = \frac{dE_\omega}{d\omega}, \tag{10}$$

A practical exploration of (10) was attempted by Gross et al. [29] who used the quasilocal density approximation (qLDA) [65] with fractional occupation numbers of the KS orbitals, although the excitation energies obtained for the He atom were unsatisfactory. Similarly poor results (with the errors on the order of a few eV) were obtained in several other works by employing various approximations for the exchange-correlation functional to calculate the excitation energies of atoms and small molecules [66–68].

Further theoretical developments of the ensemble DFT formalism for excited states were recently undertaken in [31–33]. Pernal et al. [31] demonstrated that the ensemble variational principle can be connected to the Helmholtz free-energy variational principle of the statistical mechanics. Ullrich et al. [33] used the ensemble formalism to construct the accurate exchange-correlation potentials for ensembles of ground and excited states of He atoms and several model systems that allow the exact solution (1D box and Hooke's atom). Fromager et al. [32] derived the generalized adiabatic connection formalism for ensemble DFT which can in principle provide a framework for the development of a rigorous multi-determinant DFT.

Perhaps the most significant realization in the aforementioned works on ensemble DFT is that not only the total ensemble energy E_ω but also its components should be kept linear in the ensemble weighting factors. Indeed, starting from (7) (or (5)) it is tempting to cast the ensemble energy into the traditional DFT form by splitting the energy functional into the familiar non-interacting kinetic energy T_s, the classical Hartree repulsion U_H, and the exchange-correlation E_{xc} terms, as in (11):

$$E_\omega = T_{s,\omega} + U_H[\rho_\omega] + E_{\mathrm{xc}}[\rho_\omega] + \int d^3 r v_{\mathrm{ext}}(\mathbf{r})\rho_\omega(\mathbf{r}), \tag{11}$$

where the Hartree electron–electron repulsion energy and E_{xc} are calculated for the total ensemble density,

$$U_H[\rho_\omega] = \frac{1}{2}\int d^3 r' \int d^3 r \frac{\rho_\omega(\mathbf{r})\rho_\omega(\mathbf{r}')}{|\mathbf{r} - \mathbf{r}'|}, \tag{12}$$

and a suitable approximate functional is employed for E_{xc} [29]. As the U_H energy depends nonlinearly on the density, the dependence of (12) on the ensemble weighting factors becomes nonlinear, which leads to the emergence of unphysical "ghost" contributions, i.e., cross-terms between the ensemble components. These terms are supposed to be eliminated by the XC functional, which should also become nonlinear in the ensemble weighting factors [31, 33]. The commonly available approximations for the XC functional were incapable of accurately compensating for the "ghost" contributions and, consequently, the results obtained with the use of these functionals were quite poor [29, 66–68].

Considerably better excitation energies from the ensemble DFT calculations were obtained by Pernal et al. [31], who employed a "ghost"-free formulation for the ensemble energy functional. The "ghost"-free Hartree electron–electron repulsion in [31] was calculated:

$$U_H[\rho_\omega] = \frac{1}{2}\sum_I \omega_I \int d^3r' \int d^3r \frac{\rho_I(\mathbf{r})\rho_I(\mathbf{r}')}{|\mathbf{r}-\mathbf{r}'|}, \tag{13}$$

where ρ_I are the densities of the individual components of the ensemble. In their work, Pernal et al. separated the ensemble XC energy into the long-range (lr) component which was treated at the multi-reference WFT level and the short-range (sr) XC energy approximated by a density functional:

$$E_\omega = \sum_I \omega_I \left(T_{s,I} + U_H[\rho_I] + \int d^3r\, v_{\text{ext}}(\mathbf{r})\rho_I(\mathbf{r}) + E^{lr}_{\text{xc},I} \right) + E^{\text{sr}}_{\text{xc,DFT}}[\rho_\omega]. \tag{14}$$

Although, with the use of this approach, the excitation energies of Be atom and LiH and BH molecules were considerably improved, there still remained substantial residual errors on the order of 0.6–0.8 eV. Furthermore, the sr-XC energy in (*14*) still remained nonlinear in the ensemble weighting factors and inseparable into the individual contributions of ensemble components. These shortcomings of the currently available implementations of ensemble DFT are not present in the REKS method which is described in the following section.

3 REKS Methodology

In this section the basic aspects of the REKS method are explained. The REKS method was initially developed to deal with the non-dynamic correlation in the ground electronic states of molecules [35, 38] and was later extended to treat the excited states [39–41]. The latter method is known as the state-averaged REKS (SA-REKS) [39] and the state interaction SA-REKS (SI-SA-REKS or SSR, for brevity) [40, 41].

3.1 REKS Method for Ground States

The REKS method for ground states is a practical implementation of ensemble DFT formalism that depends upon (2) and (5) [20]. Let us consider a situation that requires the use of the ensemble formalism at the DFT level and the multi-reference description at the WFT level. For instance, let us take two H_2 molecules in a rectangular arrangement as shown in Fig. 1. The $H_2 + H_2$ system was studied in [26] with the use of both the multi-reference configuration interaction (MRCI) method of WFT and the ensemble DFT formalism. In the latter case, the non-interacting KS reference state and the KS potential $v_s(\mathbf{r})$ were constructed from the MRCI density using the reverse engineering approach of Zhao, Morrison, and Parr [62]. It was found that one has to use the ensemble representation and the fractional

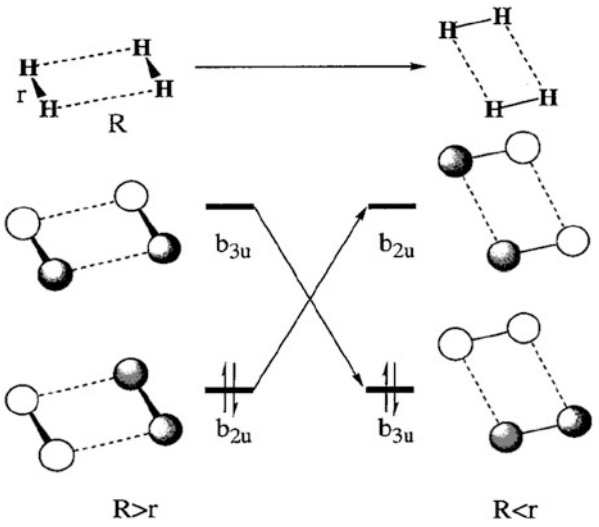

Fig. 1 Definition of geometry and frontier orbitals for the $H_2 + H_2$ system

occupations of the frontier orbitals to obtain the non-interacting KS reference system and $v_s(\mathbf{r})$ corresponding to the criteria behind the KS method of DFT; only the ensemble representation guaranteed the lowest-energy ground state of the KS system; otherwise there occurred holes below the Fermi level (not a ground state) and the resulting single determinant state lied at a somewhat higher energy [26].

At a long intermolecular separation R, the electronic structure of the system is dominated by the $(\ldots \phi_a^{(2)}\, \phi_b^{(0)})$ configuration, where ϕ_a corresponds to the b_{2u}-symmetric molecular orbital (MO) and ϕ_b to b_{3u}-symmetric MO (under the D_{2h} symmetry constraint). Such a situation is non-interacting PS-VR, i.e., it can be faithfully represented by a single KS determinant [26]. As the two molecules get closer, the gap between the highest occupied MO (HOMO) ϕ_a and the lowest unoccupied MO (LUMO) ϕ_b narrows down and, at a certain distance between the H_2 molecules, the non-dynamic correlation sets in, which is reflected in the character of the MRCI wavefunction which comprises two leading configurations, $(\ldots \phi_a^{(2)}\, \phi_b^{(0)})$ and $(\ldots \phi_a^{(0)}\, \phi_b^{(2)})$, and, at the KS DFT level, one has to switch over to the ensemble representation for the density. The frontier KS orbitals ϕ_a and ϕ_b become fractionally occupied and degenerate at the Fermi level of the system [26].

Thus, the density of the $H_2 + H_2$ system near the square conformation is given by a two-component ensemble (2) with the weighting factors λ_1 and λ_2 related to the FONs of the frontier KS orbitals, $\lambda_1 = n_a/2$ and $\lambda_2 = n_b/2$. The ensemble KS energy is given by (5) with the same weighting factors. The FONs of the frontier orbitals satisfy the condition of stationarity of the energy with respect to their variation [64]. Hence, the ensemble KS reference state obtained in [26] follows exactly theorems 4.2 and 4.3 and equations 4.5 and 4.7 of [20], and nicely illustrates the theoretical arguments behind the ensemble approach in DFT.

The ensemble KS solution obtained which comprises the densities and energies of two electronic configurations, where each is represented by a single KS determinant, corresponds to a system of non-interacting particles. To derive an energy expression that would conform with the ensemble representation and would yield the energy of a system of *interacting* electrons, let us make use of the adiabatic connection formalism [69], i.e., let us gradually switch the electron–electron interaction on and simultaneously modify the external potential in such a way that the total density remains unchanged [70]; see the Hamiltonian

$$\hat{H}_\alpha = \sum_i -\frac{1}{2}\nabla_i^2 + \sum_i v_{\mathrm{ext},\alpha}(\mathbf{r}_i) + \sum_{i>j}\frac{\alpha}{r_{ij}}, \tag{15}$$

where α is the variable coupling constant, $0 \le \alpha \le 1$, r_{ij} is the interelectronic distance, and the external potential $v_{\mathrm{ext},\alpha}$ satisfies the conditions $v_{\mathrm{ext},0} = v_s$ (the KS potential) and $v_{\mathrm{ext},1} = v_{\mathrm{ext}}$ (physical system of interacting electrons). When the electron–electron interaction is only infinitesimally switched on, such that it affects only the electrons in the degenerate orbitals at the Fermi level, the total energy with the Hamiltonian at $\alpha \approx 0$ can be obtained from quasi-degenerate perturbation theory [10] which leads to an expression which can be cast in the form of

$$\begin{aligned} E_\alpha = {} & \frac{n_a^\alpha}{2}E_\alpha\left[\ldots\phi_a\overline{\phi}_a\right] + \frac{n_b^\alpha}{2}E_\alpha\left[\ldots\phi_b\overline{\phi}_b\right] \\ & + \frac{1}{2}\left(n_a^\alpha n_b^\alpha\right)^{1/2}\left(E_\alpha[\ldots\phi_a\phi_b] - E_\alpha\left[\ldots\phi_a\overline{\phi}_b\right] + E_\alpha\left[\ldots\overline{\phi}_a\overline{\phi}_b\right] - E_\alpha\left[\ldots\overline{\phi}_a\phi_b\right]\right), \end{aligned} \tag{16}$$

where the energies of the electronic configurations are calculated using the Hamiltonian (15) and the barred orbitals and the unbarred orbitals are occupied with the beta-spin and the alpha-spin electrons, respectively. The energy term in parentheses in the second line of (16) represents the negative of the exchange integral $(\phi_a\phi_b|\phi_b\phi_a)$ expressed via the energy differences between the singlet and triplet configurations.[2]

Using the coupling strength integration [69] and making an assumption that the α-dependent occupation numbers n_a^α and n_b^α can be replaced by the respective median values, one arrives at the formula

[2] Note that the kinetic energy is independent of the spin and the total densities of the electronic configurations in the second line of (16) are identical.

$$E_{\text{ens}} = \frac{n_a}{2}E_{\text{DFT}}\left[\ldots\phi_a\overline{\phi}_a\right] + \frac{n_b}{2}E_{\text{DFT}}\left[\ldots\phi_b\overline{\phi}_b\right] + \frac{1}{2}(n_a n_b)^{1/2} \times \left(E_{\text{DFT}}[\ldots\phi_a\phi_b] - E_{\text{DFT}}\left[\ldots\phi_a\overline{\phi}_b\right] + E_{\text{DFT}}\left[\ldots\overline{\phi}_a\overline{\phi}_b\right] - E_{\text{DFT}}\left[\ldots\overline{\phi}_a\phi_b\right]\right), \tag{17}$$

where E_{DFT} denotes the total energy calculated for a single-determinant configuration using the conventional KS DFT formalism. It is noteworthy that the parenthesized term in the second line of (17) does not contribute to the total density, as the densities of these configurations cancel each other identically. Hence, the total density of a strongly correlated state can be calculated using

$$\begin{aligned}\rho_{\text{ens}} &= \frac{n_a}{2}\rho\left[\ldots\phi_a\overline{\phi}_a\right] + \frac{n_b}{2}\rho\left[\ldots\phi_b\overline{\phi}_b\right] \\ &+ \frac{1}{2}(n_a n_b)^{1/2}\left(\rho[\ldots\phi_a\phi_b] - \rho\left[\ldots\phi_a\overline{\phi}_b\right] + \rho\left[\ldots\overline{\phi}_a\overline{\phi}_b\right] - \left[\ldots\overline{\phi}_a\phi_b\right]\right), \\ &= \frac{n_a}{2}\rho\left[\ldots\phi_a\overline{\phi}_a\right] + \frac{n_b}{2}\rho\left[\ldots\phi_b\overline{\phi}_b\right]\end{aligned} \tag{18}$$

which is the weighted sum of the densities of the configurations in (17) taken with the same weighting factors.

To illustrate the derivation of (17), let us expand the ensemble energy (16) obtained from quasi-degenerate perturbation theory near $\alpha = 0$. Equation (16) is obtained as the most negative eigenvalue of the secular matrix

$$\begin{pmatrix} E_\alpha\left[\ldots\phi_a\overline{\phi}_a\right] & K^\alpha_{ab} \\ K^\alpha_{ab} & E_\alpha\left[\ldots\phi_b\overline{\phi}_b\right] \end{pmatrix}, \tag{19}$$

where $K^\alpha_{ab} = -\frac{1}{2}\left(E_\alpha[\ldots\phi_a\phi_b] - E_\alpha\left[\ldots\phi_a\overline{\phi}_b\right] + E_\alpha\left[\ldots\overline{\phi}_a\overline{\phi}_b\right] - E_\alpha\left[\ldots\overline{\phi}_a\phi_b\right]\right)$ $\left(K^\alpha_{ab} = \alpha\left(\phi_a\phi_b\middle|\phi_b\phi_a\right), \text{for } \alpha\to 0\right)$ is the coupling element between the configurations $\left|\ldots\phi_a\overline{\phi}_a\right\rangle$ and $\left|\ldots\phi_b\overline{\phi}_b\right\rangle$ (for a small α, the exchange integral between the orbitals ϕ_a and ϕ_b). Expanding this matrix with respect to α and keeping only the first term in the expansion, one obtains

(continued)

$$\begin{pmatrix} E_\alpha\left[\ldots\phi_a\overline{\phi}_a\right] & K^\alpha_{ab} \\ K^\alpha_{ab} & E_\alpha\left[\ldots\phi_b\overline{\phi}_b\right] \end{pmatrix} = \begin{pmatrix} E_0\left[\ldots\phi_a\overline{\phi}_a\right] & 0 \\ 0 & E_0\left[\ldots\phi_b\overline{\phi}_b\right] \end{pmatrix} + \alpha\begin{pmatrix} \frac{dE_\alpha\left[\ldots\phi_a\overline{\phi}_a\right]}{d\alpha} & \frac{dK^\alpha_{ab}}{d\alpha} \\ \frac{dK^\alpha_{ab}}{d\alpha} & \frac{dE_\alpha\left[\ldots\phi_b\overline{\phi}_b\right]}{d\alpha} \end{pmatrix} + O\left(\alpha^2\right), \tag{20}$$

the lowest energy solution of which is given by

$$E_\alpha = \frac{n^\alpha_a}{2}E_0\left[\ldots\phi_a\overline{\phi}_a\right] + \frac{n^\alpha_b}{2}E_0\left[\ldots\phi_b\overline{\phi}_b\right] + \alpha\left(\frac{n^\alpha_a}{2}\frac{dE_\alpha\left[\ldots\phi_a\overline{\phi}_a\right]}{d\alpha} + \frac{n^\alpha_b}{2}\frac{dE_\alpha\left[\ldots\phi_b\overline{\phi}_b\right]}{d\alpha} - \left(n^\alpha_a n^\alpha_b\right)^{1/2}\frac{dK^\alpha_{ab}}{d\alpha}\right). \tag{21}$$

In (21), it was used that $E_0\left[\ldots\phi_a\overline{\phi}_a\right] = E_0\left[\ldots\phi_b\overline{\phi}_b\right]$ and $n^\alpha_a + n^\alpha_b = 2$, where the occupation numbers $n^\alpha_a = 2\left|c^\alpha_1\right|^2$ and $n^\alpha_b = 2\left|c^\alpha_2\right|^2$ are obtained from the lowest eigenvector (c^α_1, c^α_2) of the matrix in the second line of (20).

Assuming that the occupation numbers n^α_a and n^α_b can be replaced by their respective median values, n_a and n_b, and performing the usual coupling constant integration [69, 70], one arrives at

$$E_{\text{ens}} = \frac{n_a}{2}E_0\left[\ldots\phi_a\overline{\phi}_a\right] + \frac{n_b}{2}E_0\left[\ldots\phi_b\overline{\phi}_b\right] + \int\rho_{\text{ens}}(\mathbf{r})(\nu_{\text{ext},1}(\mathbf{r}) - \nu_{\text{ext},0}(\mathbf{r}))d\mathbf{r} + \frac{n_a}{2}E_{\text{Hxc}}\left[\ldots\phi_a\overline{\phi}_a\right] + \frac{n_b}{2}E_{\text{Hxc}}\left[\ldots\phi_b\overline{\phi}_b\right] + \frac{1}{2}(n_a n_b)^{1/2} \times\left(E_{\text{Hxc}}\left[\ldots\phi_a\overline{\phi}_b\right] - E_{\text{Hxc}}\left[\ldots\phi_a\overline{\phi}_b\right] + E_{\text{Hxc}}\left[\ldots\overline{\phi}_a\overline{\phi}_b\right] - E_{\text{Hxc}}\left[\ldots\overline{\phi}_a\phi_b\right]\right), \tag{22}$$

where the E_{Hxc} terms comprise the Hartree and the XC energy of the given configuration. Equation (17) is obtained from (22) using the density ρ_{ens} in (18) and noting that the sum of the kinetic energy and the interaction with the external potential $v_{\text{ext},1}$ is the same for the four terms in parentheses in the third line of (22). When deriving (17), it was also assumed that no further degeneracies (except the point $\alpha = 0$) occur along the adiabatic connection path.

The formulae obtained for the density and the energy are valid for the case of strong non-dynamic correlation, where the occupation numbers of the fractionally occupied orbitals are close to unity, $n_a \approx n_b \approx 1$. When the multi-reference

character of the system subsides to a level commensurate with the pure-state v-representability, the ensemble energy in (17) should collapse to the usual KS DFT single-reference energy. Analyzing the dependence of the single-reference KS DFT energy on the FONs of the frontier orbitals near, say, $n_a \approx 2$ and $n_b \approx 0$, an expression similar to (17) can be obtained with the difference that the factor $(n_a n_b)^{1/2}$ approaches $(n_a n_b)^1$ [71, 72]. It is thus plausible to introduce a function that interpolates between the two asymptotes, the strong and the weak non-dynamic correlation, and to cast (17) in the form of [35]

$$E^{\mathrm{REKS}(2,2)} = \frac{n_a}{2} E_{\mathrm{DFT}}\left[\ldots \phi_a \overline{\phi}_a\right] + \frac{n_b}{2} E_{\mathrm{DFT}}\left[\ldots \phi_b \overline{\phi}_b\right] + f(n_a, n_b)\left(E_{\mathrm{DFT}}[\ldots \phi_a \phi_b] - E_{\mathrm{DFT}}\left[\ldots \phi_a \overline{\phi}_b\right] + E_{\mathrm{DFT}}\left[\ldots \overline{\phi}_a \overline{\phi}_b\right] - E_{\mathrm{DFT}}\left[\ldots \overline{\phi}_a \phi_b\right]\right), \tag{23}$$

where $f(n_a,n_b)$ is the interpolating function defined in [38]:

$$f(n_a, n_b) = \frac{1}{2}(n_a n_b)^{1-\frac{1}{2}\frac{n_a n_b + \delta}{1+\delta}}. \tag{24}$$

The damping factor in (24) is set to a value $\delta = 0.4$ to provide for a stable convergence of the REKS self-consistent field (SCF) iterations near the regime when E-VR solution collapses to the PS-VR solution [73]. In the described version of REKS, the FONs of the two frontier orbitals are restricted to sum up to two electrons; hence the name REKS(2,2), which is similar to the notation adopted for the complete active space SCF (CASSCF) method in multi-reference WFT.

In the strict implementation of KS theory, the derived REKS total energy should be minimized with respect to the REKS density (naturally, the FONs too). As the REKS energy is not an explicit functional of the density, such a minimization should inevitably rely on a variant of the optimized effective potential (OEP) approach [74], which is known to suffer from steep computation time scaling and certain stability issues when used in connection with the localized basis sets for expanding the KS orbitals [75]. Therefore, the REKS total energy is minimized with respect to the orbitals, as is being commonly done in connection with the hybrid and meta GGA density functionals, thus avoiding the need to tackle the density–density response function[3] used in the OEP formalism. The FONs are obtained variationally by minimizing the energy (23) under the constraint $n_a + n_b = 2$. The latter constraint is imposed explicitly, without using the method of Lagrange multipliers. The REKS orbitals are optimized using the coupling operator technique of the open-shell SCF theory [77]. For brevity, the REKS one-electron equations are not presented here and the reader is referred to the original publications [34, 35, 43]; see also a review article [73].

[3] See [76] for the derivation of density–density response function for ensemble densities.

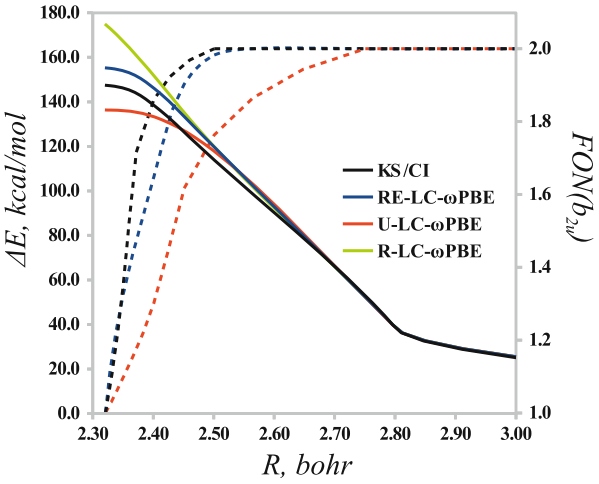

Fig. 2 Profile of the PES of $H_2 + H_2$ reaction and populations of the b_{2u} orbital as obtained from the KS/CI (*black*), BS-UKS (*red*), RKS (*green*), and REKS (*blue*) calculations. The relative energies are calculated with respect to two isolated H_2 molecules. *Solid curves* show the energies and *dashed curves* show the occupation numbers as a function of R (see Fig. 1 for definition). DFT calculations employ the LC-ωPBE functional

The derived REKS energy expression is based on a number of assumptions, of which the most severe is perhaps the assumption that the coupling strength dependent occupation numbers n_i^α in (16) can be replaced by their median values n_i in (17) to avoid the need to carry out their integration with respect to α. Although the coupling strength integration of the ensemble weighting factors for partially interacting Hamiltonians was attempted by Fromager et al. when deriving the generalized adiabatic connection for ensemble DFT [32], to keep the formalism simple we prefer to stick to the above assumption and to verify whether it is sufficiently accurate by comparing the results obtained using the REKS method with the reference (exact) data. In the following, an example is presented that illustrates the validity of the above assumptions.

The $H_2 + H_2$ reaction studied by Schipper et al. [26] is perhaps the simplest example of a 2+2 symmetry forbidden cycloaddition reaction [78–80]. This reaction was investigated using the MRCI/cc-pV5Z method and the ensemble KS reference was obtained from the MRCI density [26]. The potential energy surface (PES) profile along the direction of approach of the two H_2 molecules (see Fig. 1 for definitions) is shown in Fig. 2 along with the b_{2u} orbital population as obtained in the MRCI and DFT calculations. The DFT calculations in Fig. 2 employ the LC-ωPBE [81–83] range-separated density functional and three different computational techniques: the REKS method, the broken-symmetry spin-unrestricted KS (BS-UKS) method, and the conventional single-reference spin-restricted KS (RKS) method. All three DFT methods yield the same energy (−2.3574534 a.u.) for the two H_2 molecules at long distance from one another.

The RKS method fails to take proper account of the non-dynamic correlation arising from (near) degeneracy of the $(\ldots b_{2u}^{(2)} b_{3u}^{(0)})$ and $(\ldots b_{2u}^{(0)} b_{3u}^{(2)})$ configurations in the vicinity of the barrier summit and yields a cusp on the PES instead of a smooth transition state. The BS-UKS and REKS methods yield a smooth transition

between the configurations, although the BS-UKS curve deviates stronger from the target MRCI PES and underestimates the reaction barrier height. The FONs of the frontier orbitals (only the b_{2u} FON shown in Fig. 2) obtained by the REKS method are in a good agreement with the exact ensemble KS values, whereas the BS-UKS occupations (the natural orbital's occupation numbers are shown in lieu of FONs) deviate strongly from the exact ones, suggesting that BS-UKS overestimates the effect of the non-dynamic correlation. Furthermore, BS-UKS displays an abrupt onset of the non-dynamic correlation (after ca. $R = 2.75$ bohr), whereas the REKS method yields a smooth transition between the PS-VR and E-VR regimes and a more accurate description of the reaction PES profile.

The comparison vis-à-vis the exact ensemble KS results demonstrates the validity of the approximations made in the REKS working equations. Besides the $H_2 + H_2$ system, the REKS method was applied to study bond-breaking/bond-formation reactions in several chemical systems as well as the electronic structure of biradicals, magnetic coupling in metal complexes and organic charge transfer crystals. The reader is advised to inspect the original publications [37, 38, 42–53, 56, 57] for more examples of the method performance.

3.2 REKS Method for Excited States: SA-REKS and SI-SA-REKS

Let us consider a model system with two strongly correlated electrons in two orbitals, such as the H_2 molecule with the bond stretched beyond the Coulson–Fischer point [84]. Near the equilibrium bondlength, the electronic structure of H_2 is dominated by a single configuration $\left|1\sigma_g 1\overline{\sigma}_g\right\rangle$ and the doubly excited configuration $|1\sigma_u 1\overline{\sigma}_u\rangle$ lies high in energy ($1\sigma_g$ is the bonding MO and $1\sigma_u$ the anti-bonding MO). When the bond is stretched beyond the Coulson–Fischer point, the energy gap between the two electronic configurations narrows to a limit that allows for an efficient mixing of the configurations and the strong non-dynamic electron correlation ensues. In the minimal basis of the two orbitals (the bonding $1\sigma_g$ MO denoted to ϕ_a and the anti-bonding $1\sigma_u$ to ϕ_b), the ground-state wavefunction of stretched H_2 can be represented by a two-configurational wavefunction:

$$\Phi_0 = \sqrt{\frac{n_a}{2}}|\phi_a\overline{\phi}_a\rangle - \sqrt{\frac{n_b}{2}}|\phi_b\overline{\phi}_b\rangle, \tag{25}$$

where n_a and n_b are the FONs of the orbitals ϕ_a and ϕ_b. Promoting a single electron from ϕ_a to ϕ_b orbital leads to a singlet excited state Φ_1 which can be represented by the wavefunction

$$\Phi_1 = \frac{1}{\sqrt{2}}|\phi_a\overline{\phi}_b\rangle + \frac{1}{\sqrt{2}}|\phi_b\overline{\phi}_a\rangle, \tag{26}$$

For a homosymmetric molecule, such as H_2, the two states belong in different symmetry species and therefore do not interact with one another.

Using the ensemble DFT for excited states, described in Sect. 3.1, the excitation energy can be obtained from the variational optimization of the energy of an ensemble of the two states [5]. The ground state (25) can be described by the REKS(2,2) method and the excited state (26) by the spin-restricted open-shell KS (ROKS) method for an open-shell singlet (OSS) state [12, 34]. Within the latter approach, the energy of the OSS state is given by [12, 34]

$$E^{\text{ROKS}} = E_{\text{DFT}}\left[\ldots\phi_a\overline{\phi}_b\right] - \frac{1}{2}E_{\text{DFT}}\left[\ldots\phi_a\phi_b\right] + E_{\text{DFT}}\left[\ldots\overline{\phi}_a\phi_b\right] - \frac{1}{2}E_{\text{DFT}}\left[\ldots\overline{\phi}_a\overline{\phi}_b\right]. \tag{27}$$

The use of the REKS and ROKS energies in (7) leads to the SA-REKS energy expression [39]:

$$E_\omega^{\text{SA-REKS}} = (1-\omega)E^{\text{REKS(2,2)}} + \omega E^{\text{ROKS}}, \tag{28}$$

which is to be variationally optimized with respect to the density of the ensemble of the two states. Similar to the REKS(2,2) method, and to save the computational effort, the minimization with respect to the density is replaced by the minimization with respect to the orbitals and the orbitals' FONs (in the REKS(2,2) energy) [39]. Typically, equal weighting factors, i.e., $\omega = 1/2$, are employed in practical calculations with the SA-REKS method. Having completed the orbital optimization (carried out by the same open-shell SCF method as used in the ground-state REKS calculations) [73], the energies of the individual states are calculated using the common set of orbitals and the excitation energy is obtained by (9).

Let us illustrate how the SA-REKS method works by applying it to the H_2 molecule at varying bondlengths. Aryasetiawan et al. [9] found that the LR-TD-DFT approach in the adiabatic approximation is incapable of correctly describing the dependence of the ${}^1\Sigma_u^+ \leftarrow {}^1\Sigma_g^+$ excitation energy of H_2 on the bondlength. Figure 3 compares the exact excitation energy obtained from the data of [85] with the results of the TD-DFT and SA-REKS calculations carried out using the LC-ωPBE density functional and the cc-pV5Z basis set. Although the SA-REKS excitation energy curve in the lower panel of Fig. 3 is slightly shifted down with respect to the exact curve (the magnitude of the shift is dependent on the XC functional employed), it follows the shape of the exact curve sufficiently accurately and has a shallow minimum around $R_{\text{HH}} = 4.0$ bohr, which is comparable to the exact curve that minimizes at $R_{\text{HH}} = 4.1$ bohr. The adiabatic TD-DFT excitation energy curve does not have a minimum and, at long H–H bondlengths, goes

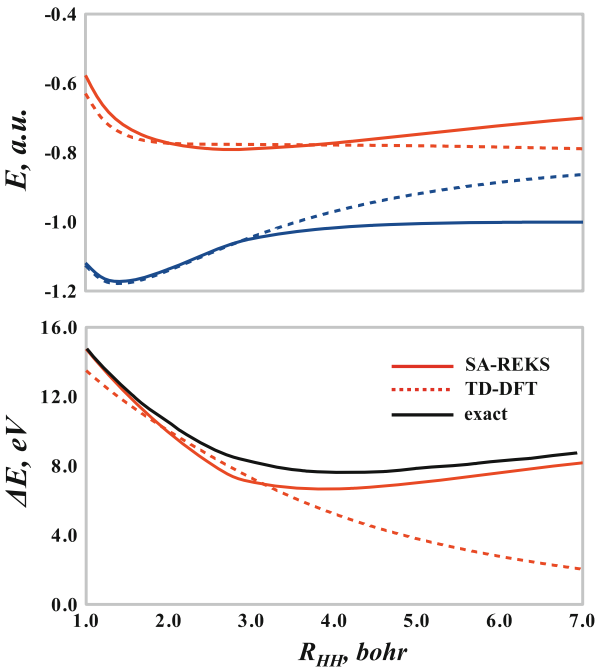

Fig. 3 Potential energy curves (*upper panel*) of the ${}^1\Sigma_g^+$ and ${}^1\Sigma_u^+$ states of H_2 and the ${}^1\Sigma_u^+ \leftarrow {}^1\Sigma_g^+$ excitation energy (*lower panel*) as a function of the H–H distance. *Solid colored curves* (*blue* for the ground state and *red* for the excited state) represent the results of the SA-REKS calculations, *dashed colored curves* refer to TD-DFT, and the *black curve* is the exact excitation energy from [85]. DFT calculations employ the LC-ωPBE density functional and the cc-pV5Z basis set

gradually to zero. As seen in the upper panel of Fig. 3, the SA-REKS method correctly describes the H–H bond dissociation, whereas the single-reference RKS approach fails to yield the correct dissociation limit for the H_2 molecule. Thus, it is the failure of the conventional KS DFT approach to describe the non-dynamic electron correlation for a dissociating covalent bond that is responsible for the failure of TD-DFT to describe correctly the excitation energy of a dissociating molecule.

The described SA-REKS method is capable of describing the ground and excited states of a homosymmetric molecule when the mixing of the two states is prevented by symmetry. In the case of a heterosymmetric molecule, e.g., dissociating LiH, the two states in (25) and (26) are allowed to mix and therefore their representation as a purely covalent state and a purely ionic state is no longer accurate. To correct for this deficiency of the SA-REKS description and to construct an ensemble of two decoupled states, one can obtain a pair of new states by solving a 2×2 secular problem with the Hamiltonian matrix that spans the $E^{\mathrm{REKS}(2,2)}$ and the E^{ROKS} energies as the diagonal elements and the off-diagonal (coupling) element given in (29):

$$H_{01} = \sqrt{n_a}\langle\phi_b|n_a\hat{F}_a|\phi_a\rangle - \sqrt{n_b}\langle\phi_a|n_b\hat{F}_b|\phi_b\rangle = (\sqrt{n_a} - \sqrt{n_b})\varepsilon_{ab} \qquad (29)$$

which was obtained in [40, 41] by applying the Slater–Condon rules in the space of the two CSFs Φ_0 and Φ_1 and the variational condition for the open-shell orbitals ϕ_a

and ϕ_b [34, 35, 77]. In (29), $\hat{F}_a$ and $\hat{F}_b$ are the Fock operators for the open-shell orbitals and ε_{ab} is the off-diagonal Lagrange multiplier[4] in the open-shell Lagrangian [73]. As the two states, Φ_0 and Φ_1, are mutually orthogonal, the average of the new energies E_0 and E_1 obtained from the above secular problem remains the same as the average of the REKS(2,2) and ROKS energies. This implies that the orbitals for the new approach, dubbed SI-SA-REKS or SSR, can still be obtained from the SA-REKS orbital optimization, provided that $\omega = 1/2$ was employed in the latter. In practical applications of the SI-SA-REKS method [40, 41, 59–61], it was found that the described state-interaction scheme is important for obtaining the correct shape of the ground and excited state PESs in the vicinity of conical intersections and near avoided crossings. For other situations, when the energy gap between the ground and excited states is sufficiently wide the SI-SA-REKS method yields nearly the same excitation energies as the SA-REKS method [59].

The argument leading to the SI-SA-REKS method can be proposed based on the adiabatic connection formalism for ensemble DFT as advocated by Fromager et al. [32]. Setting the coupling strength α in the Hamiltonian (15) to zero leads to the degeneracy of the states represented by (25) and (26). Applying the quasi-degenerate perturbation theory results in a 2×2 secular problem $\begin{pmatrix} E_0^\alpha & H_{01}^\alpha \\ H_{10}^\alpha & E_1^\alpha \end{pmatrix}$, where the off-diagonal elements are given by (29) for the intermediate coupling strength. Employing the coupling strength integration and invoking the assumptions used in (22) one arrives at the energy expressions for the ground and excited states of the SI-SA-REKS method (see the paragraph above). It should be noted that, for a homosymmetric molecule, such as H_2, the off-diagonal matrix element vanishes by symmetry and the SI-SA-REKS description collapses to the SA-REKS one.

To illustrate how the SI-SA-REKS method describes dissociation of a heteropolar chemical bond, let us briefly review the ground and the lowest excited singlet states of the LiH molecule. Near the equilibrium bondlength, the ground state of the LiH molecule has ionic character with ca. 0.3 $\bar{e}$ shifted to the hydrogen atom. When the Li–H bond dissociates, the ground state undergoes an avoided crossing with the excited state, which has covalent character, and, at the dissociation limit, the ground state corresponds to a covalent configuration with two electrically neutral atoms.

The potential energy curves of the ground $x^1\Sigma^+$ and the excited $a^1\Sigma^+$ states of LiH are shown in Fig. 4. The results of the SI-SA-REKS calculations using the LC-

[4] The matrix of Lagrange multipliers in open-shell SCF becomes Hermitian (but not diagonal) upon convergence to the variational minimum [77].

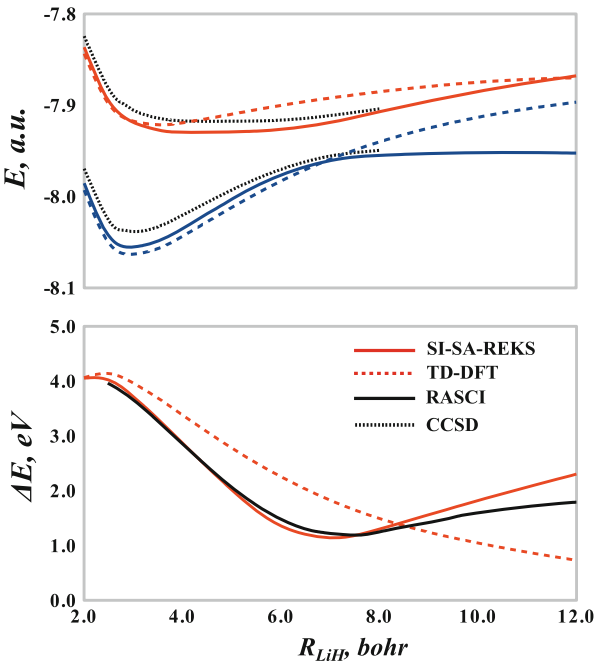

Fig. 4 Potential energy curves (*upper panel*) of the $x^1\Sigma^+$ and $a^1\Sigma^+$ states of LiH and the $x^1\Sigma^+ \leftarrow a^1\Sigma^+$ excitation energy (*lower panel*) as a function of the Li-H distance. *Solid curves* – SI-SA-REKS results, *dashed curves* – TD-DFT results. DFT calculations employ the LC-ωPBE functional and aug-cc-pVTZ basis set. *Solid black curve* in the lower panel shows the reference RASCI excitation energy [86] and the *dotted black curves* in the upper panel show the CCSD energies [31] of the two states

ωPBE functional and the aug-cc-pVTZ basis set are compared with the results of the conventional TD-DFT calculations (with the same basis set and functional) and with the literature data. The $x^1\Sigma^+ \leftarrow a^1\Sigma^+$ excitation energy of LiH was recently studied using an ab initio restricted active space CI (RASCI) method with the aug-cc-pVTZ basis set [86]. For the individual states, the $x^1\Sigma^+$ and the $a^1\Sigma^+$ states, the potential energy curves along the dissociation path were obtained in [31] using the CCSD method (presumably the EOM-CCSD was used to obtain the excited state curve).

As seen in Fig. 4, the SI-SA-REKS potential energy curves follow closely the ab initio results, whereas the conventional KS DFT curves fail to reproduce the correct dependence on distance. Near ca. $R_{\mathrm{LiH}} = 7$ bohr, the two states undergo an avoided crossing as seen in the curves obtained by the ab initio WFT calculations and the SI-SA-REKS calculations. The RKS ground-state curve does not converge to the correct dissociation limit and the ground state remains ionic along the whole dissociation path. The excitation energy from the SI-SA-REKS calculations closely follows the RASCI excitation energy curve and correctly yields the avoided crossing. The TD-DFT excitation energy, although close to the ab initio value near the equilibrium distance, fails to display the correct distance dependence and vanishes at the dissociation limit. This example illustrates yet another failure of the conventional KS DFT/TD-DFT approach to describe the ground and excited state potential energy surfaces of molecules with dissociating bonds (or, more generally, strongly correlated molecular systems). By contrast, the SI-SA-REKS method describes these situations with high accuracy and can be applied with confidence to study the excited states of strongly correlated molecules.

4 Applications of the REKS Method to Excited States

Although the application of the SA-REKS and SI-SA-REKS methods to diatomic molecules in Sect. 3.2 illustrates their capabilities in comparison with the (nearly) exact calculations, a more general benchmarking of the methods is needed to establish them as generally applicable computational schemes. In [59], the accuracy of the SI-SA-REKS method for valence excitations in ordinary (i.e., not strongly correlated) organic molecules was studied. For a set of 15 $\pi \rightarrow \pi^*$ and $n \rightarrow \pi^*$ excitations in aliphatic and aromatic hydrocarbons, it was found that SI-SA-REKS describes these excitations on a par with the widely used linear response methods, such as TD-DFT or ADC(2) [87–91] (second-order algebraic diagrammatic construction; a method based on second-order perturbation expansion of the linear-response polarization propagator).

Table 1 compares the results of the SI-SA-REKS calculations carried out with the BH&HLYP and LC-ωPBE functionals in connection with the aug-cc-pVTZ basis set with the traditional TD-DFT calculations and the best estimates of vertical excitation energies from [92]. The mean absolute deviation (MAD) shown by SI-SA-REKS is nearly the same as for the TD-DFT method with the same density functional. The ab initio WFT technique ADC(2) shows for the same excitation energies a mean deviation of 0.43 eV. These benchmarks show that the SI-SA-

Table 1 The $\pi \rightarrow \pi^*$ and $n \rightarrow \pi^*$ electronic excitation energies (eV) of organic molecules. Symmetry of the excited state is given parenthetically. MAD stands for "mean absolute deviation." All calculations employ the aug-cc-pVTZ basis set

			BH&HLYP[b]		LC-ωPBE[b]	
Molecule	Transition	Best estm.[a]	TD	SSR	TD	SSR
Ethylene	$\pi \rightarrow \pi^*(^1B_{1u})$	7.80	6.93	7.37	7.61	7.61
Butadiene	$\pi \rightarrow \pi^*(^1B_u)$	6.18	5.75	5.59	5.95	5.98
Hexatriene	$\pi \rightarrow \pi^*(^1B_u)$	5.10	4.83	4.64	5.03	5.11
Octatetraene	$\pi \rightarrow \pi^*(^1B_u)$	4.66	4.21	4.01	4.43	4.54
Cyclopropene	$\pi \rightarrow \pi^*(^1B_2)$	7.06	6.28	6.54	6.41	6.57
Cyclopentadiene	$\pi \rightarrow \pi^*(^1B_2)$	5.55	5.05	5.13	5.25	5.23
Norbornadiene	$\pi \rightarrow \pi^*(^1A_2)$	5.34	5.04	5.08	5.37	5.30
Furan	$\pi \rightarrow \pi^*(^1B_2)$	6.32	5.82	6.02	6.20	6.28
Pyrrole	$\pi \rightarrow \pi^*(^1B_2)$	6.57	6.08	6.03	6.35	6.48
Imidazole	$\pi \rightarrow \pi^*(^1A')$	6.19	6.33	6.30	6.56	6.58
	$n \rightarrow \pi^*(^1A'')$	6.81	7.02	6.87	6.86	6.81
Pyridine	$\pi \rightarrow \pi^*(^1B_2)$	4.85	5.64	5.91	5.54	6.24
	$n \rightarrow \pi^*(^1B_1)$	4.59	5.26	5.18	5.17	5.04
Uracil	$\pi \rightarrow \pi^*(^1A')$	5.35	5.54	5.53	5.49	5.71
	$n \rightarrow \pi^*(^1A'')$	4.80	5.26	5.13	5.12	5.20
MAD			0.47	0.43	0.28	0.30

[a]Best estimates of vertical excitation energies from [92]
[b]Geometries are taken from [92]

REKS method can be used as a general purpose computational scheme for describing the valence excitation energies.

Obviously, the ability of the SI-SA-REKS method to describe electronic transitions in strongly correlated molecules enables one to apply this method beyond the realm of applicability of the conventional adiabatic linear-response TD-DFT. Thus, the method was employed to study the optically bright ^1L_a electronic transitions ($^1B_{1u}$ symmetry) in a series of linear *n*-acenes (**1**) [59].

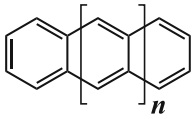

1

These transitions can be accurately described as HOMO → LUMO one-electron transitions and for a few members of the polyacene series the excitation energies were obtained experimentally either in the gas phase (or in solution and corrected for the solvent effects) or in inert gas matrices (see [59] and references cited therein). It was estimated that, with the growing number of fused rings, the ^1L_a excitation energy flattens out at a value of 1.18 ± 0.06 eV extrapolated in [93] from the matrix isolation values.

The results of the SI-SA-REKS calculations are compared in Table 2 with the TD-DFT results and the available experimental data. The TD-DFT excitation energies gradually approach zero as the number of fused rings increases. This

Table 2 ^1L_a ($^1B_{1u}$) excitation energy (eV) of polyacenes. The6-311 + G(2d,p) basis set is employed in DFT calculations

		BH&HLYP[b]		CAM-B3LYP[b]	
Molecule	Exp.[a]	TD	SSR	TD	SSR
Naphthalene	4.44	4.61	4.82	4.56	4.67
Anthracene	3.41	3.48	3.64	3.49	3.55
Tetracene	2.76	2.70	2.85	2.73	2.81
Pentacene	2.21	2.15	2.29	2.19	2.29
Hexacene	1.89	1.73	1.89	1.79	1.91
Heptacene	1.70	1.40	1.57	1.47	1.61
Octacene	1.54	1.11	1.35	1.20	1.40
Nonacene	1.43	0.89	1.20	1.00	1.26
Decacene		0.72	1.11	0.83	1.16
Dodecacene		0.45	1.00	0.59	1.05
Tetradecacene		0.22	0.95	0.40	0.99
Hexadecacene		0.10	0.92	0.29	0.95
Octadecacene		0.19	0.89	0.22	0.93
Icosacene		0.22	0.87	0.17	0.90

[a]Experimental gas phase or matrix isolation excitation energies cited in [59]

[b]Geometries were optimized in [59] using the RE-B3LYP/6-31G* method

feature of TD-DFT excitation energies is independent of the density functional employed (see [59] for more detail) and is another illustration of the failure of the conventional KS DFT approach to strongly correlated systems.

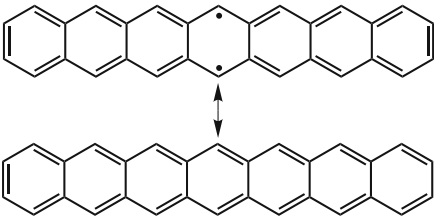

Polyacenes are known to have a strongly correlated ground state and this is illustrated by a sketch of the valence Lewis structures in the diagram above [94]. Therefore the use of multi-reference approaches is mandatory for proper description of their ground state. The single-reference KS DFT is incapable of taking accurate account of the non-dynamic correlation in the ground state of longer polyacenes and the TD-DFT excitation energies become unrealistically low for these molecules. The SI-SA-REKS method describes accurately the ground state of polyacenes and yields excitation energies in good agreement with the experimental figures.

Another situation where the description of the non-dynamic correlation in the ground state becomes important is the real crossing between the ground and lowest excited states of the same spin and space symmetry, the so-called conical intersections. The SI-SA-REKS method was successfully applied to study conical intersections in a series of organic molecules and models of biological chromophores [40, 41, 60, 95], molecular switches [55], and molecular motors [54, 58, 61]. In these applications and benchmarks, the SI-SA-REKS method was capable of describing the geometry at the minimum of the conical intersection seam (the so-called minimum energy conical intersection, MECI) with an accuracy matching high level ab initio multi-reference methods such as MRCI and CASPT2. The results of the application of SI-SA-REKS to conical intersections are described in another chapter of this book;[5] here it is only mentioned that the root mean square deviation of the SI-SA-REKS MECI geometries from the ab initio reference geometries is less than 0.1 Å on average (0.0609 Å was obtained in [95] for a set of 12 MECIs).

Besides being capable of describing excitations of strongly correlated molecular species, the SI-SA-REKS method displays an outstanding performance in other situations which proved to be difficult for standard linear response methods.

[5] See the chapter "Description of conical intersections with density functional methods" by M. Huix-Rotllant, A. Nikiforov, W. Thiel, and M. Filatov.

Table 3 Lowest electronic excitation energy (eV) of cyanine dyes. The aug-cc-pVTZ basis set is employed in DFT calculations

	BH&HLYP[a]		CAM-B3LYP[a]			
Molecule	TD	SSR	TD	SSR	CASPT2[b]	DMC[b]
CN5	5.35	4.87	5.19	4.71	4.69	5.03
CN7	4.19	3.72	4.07	3.65	3.52	3.83
CN9	3.49	3.06	3.39	3.03	2.81	3.09
CN11	3.02	2.62	2.93	2.62	2.46	2.62

[a]Geometries are taken from [96]
[b]CASPT2 and diffusion Monte–Carlo (DMC) data from [101]

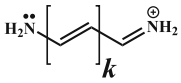

2

In cyanine dyes (**2**), the lowest singlet $^1B_1$ (in C_{2v} symmetry) excited state ($\pi \rightarrow \pi^*$ transition) is notoriously difficult for linear response methods [96–98]. TD-DFT with the commonly available density functionals overestimates the excitation energies by ca. 0.4–0.5 eV; this deviates from the trend typical for TD-DFT which has a tendency to underestimate the valence excitation energies by ca. 0.3–0.4 eV. The cyanine dyes do not have a strongly correlated ground state and it was the incorrect description of the differential correlation effects between the ground and excited states that was blamed for the poor performance of TD-DFT [99]. However, this conjecture was challenged by Ziegler et al. [100] who showed that going beyond the linear response approximation leads to considerable improvement of the calculated excitation energies.[6]

The $^1B_1$ excitation energies in a series of cyanine dyes were studied in [59] with the use of the SI-SA-REKS method in connection with a few commonly available density functionals and the aug-cc-pVTZ basis set. The results of the SI-SA-REKS calculations are compared in Table 3 with TD-DFT and with a number of high level ab initio calculations, the second-order complete active space perturbation theory (CASPT2), and the diffusion Monte–Carlo (DMC) calculations from [96]. The results in Table 3 show that SI-SA-REKS noticeably outperforms TD-DFT in the accuracy of description of the target excitation energies, thus demonstrating the advantage of the ensemble formalism. Indeed, the KS orbitals in the SI-SA-REKS method are variationally optimized for both states, the ground and the excited state, and the good performance of SI-SA-REKS seems to agree with the conclusions of Ziegler et al. [100, 102] drawn from the results of the application of the relaxed constricted variational DFT (RSCF-CV(∞)-DFT) method, a method that goes beyond the linear response and affords a variational optimization of the orbitals

[6] See the chapter "A Constricted Variational Density Functional Theory Approach to the Description of Excited States" by T. Ziegler, M. Krykunov, I. Seidu, and Y. C. Park.

Table 4 Excitation energies (eV) of the lowest CT transitions of the Ar-TCNE adducts. The cc-pVDZ basis set is employed in all DFT calculations

	BLYP[a]		BH&HLYP[a]		LC-ωPBE[a]			
Arene	TD	SSR	TD	SSR	TD	SSR	Lit.[b]	Exp.[c]
Benzene	1.54	3.53	2.96	3.52	4.00	3.69	3.80	3.59
Naphthalene	0.34	2.28	1.84	2.46	3.01	2.74	2.70	2.60
Toluene	1.37	2.72	2.67	3.26	3.65	3.30	3.40	3.36
o-Xylene	1.47	2.61	2.42	2.85	3.40	3.01	3.00	3.15
MAD[d]	2.00	0.39	0.70	0.15	0.34	0.11	0.13	

[a]Geometries are taken from [101]
[b]Literature data: results of TD-DFT calculations using the tuned range separated BNL functional from [101]
[c]Gas phase excitation energies of CT transitions from [106]
[d]Mean absolute deviations from the experimental data

partaking in the electronic transition [100, 102]. The SI-SA-REKS method achieves the same effect by using the ensemble formalism.

The use of ensemble formalism based on the variational principle also turns out to be beneficial for the description of charge transfer transitions. Linear response methods, such as TD-DFT, experience considerable difficulties when describing this type of electronic excitation, especially when used in connection with the commonly available approximate density functionals [103, 104]. Although it was not designed with these particular excitations in mind, the SI-SA-REKS method was found to be surprisingly accurate for charge transfer excitations, even when used in connection with the stock parameterization of the commonly available GGA and hybrid density functionals [105].

Table 4 reports excitation energies of the lowest charge transfer transitions of a series of arene–TCNE (tetracyanoethylene) adducts, for which the gas phase optical absorption spectra are available [106]. For these electronic transitions, the TD-DFT excitation energies obtained with the use of the usual density functionals deviate from the experimental figures by a wide margin and only the use of individually tuned range-separated density functionals brings these errors down to an acceptable level [101]. However, the accuracy achieved with the fine-tuned density functionals is easily surpassed by the SI-SA-REKS method employed in connection with the standard parameterizations of commonly available density functionals. Even when used in connection with the GGA functional, such as BLYP, the SI-SA-REKS method yields more accurate charge transfer excitation energies than does TD-DFT with the use of range-separated hybrid functional (see Table 4). The observed excellent performance of SI-SA-REKS is consistent with the analysis of the description of various types of excitations undertaken by Ziegler et al. [100, 104] who showed that it is the use of approximate density functionals in connection with the adiabatic linear response approximation that is to blame for ludicrous performance of the adiabatic TD-DFT and not the density functional alone.

To conclude this section, ensemble DFT for excited states as implemented in the SI-SA-REKS method is a versatile and accurate approach to the calculation of

various types of excitations in molecular systems. A wide range of excited states, which are otherwise inaccessible with the use of TD-DFT, can be studied, including the charge transfer excitations [105], excitations in extended π-conjugated systems [59], excitations in molecules undergoing bond breaking/bond formation [39], conical intersections between the ground and excited electronic states [40, 41, 54, 55, 58, 60, 61, 95], etc. It is also noteworthy that the SI-SA-REKS results can be obtained at an essentially mean-field cost, avoiding a steeper scaling of the linear response formalism of TD-DFT.

5 Conclusions and Outlook

Ensemble DFT [18, 20, 21, 23, 29] holds considerable promise for theoretical description of the excited states of strongly correlated molecular systems. Although it was conceived more than three decades ago, ensemble DFT still did not find its way to the repertoire of the methods used by computational chemists on a daily basis. Perhaps it is the perceived lack of practical implementations of ensemble DFT that holds down its adoption by a wider computational chemistry community. Although there is a renewed interest in developing ensemble DFT further [31–33] and in implementing it in the form of practically affordable computational schemes, these approaches are largely unknown to ordinary computational chemists.

The REKS computational method, reviewed in this chapter, makes ensemble DFT affordable. The method has already been used to study various types of electronic transitions occurring in usual as well as strongly correlated molecular systems and its ability to describe excitation energies in these systems with a remarkable accuracy has been demonstrated. Although the currently available implementation of the REKS formalism is not free of certain limitations, in particular the size of the active space and the number of excited states are restricted, these limitations will be removed in the near future and this should considerably improve the prospects for practical use of the method. Especially promising for obtaining multiple excited states and for simulating the entire excitation spectra of strongly correlated molecules appears to be a merger of the REKS methodology with the variational constricted DFT formalism proposed by Ziegler et al. [102, 104] (see Footnote 6). The work in these directions is currently in progress and will continue in the future.

References

1. Hohenberg P, Kohn W (1964) Phys Rev 136:B864
2. Kohn W, Sham LJ (1965) Phys Rev 140:A1133
3. Casida ME, Jamorski C, Bohr F, Guan JG, Salahub DR (1994) In: Karna SP, Yeates AT (eds) Nonlinear optical materials: theory and modeling, ACS symposium series, vol. 628, (Am Chem Soc, Div Comp Chem, 1996), ACS Symposium Series, vol. 628, pp 145–163.

Symposium on nonlinear optical materials – theory and modeling, at the 208th National Meeting of the American Chemical Society, Washington, DC
4. Casida ME, Huix-Rotllant M (2012) Annu Rev Phys Chem 63:287
5. Marques MAL, Gross EKU (2003) In: Fiolhais C, Nogueira F, Marques MAL (eds) A primer in density-functional theory, lecture notes in physics, vol 620. Springer, Berlin, pp 144–184
6. Maitra NT, Zhang F, Cave R, Burke K (2004) J Chem Phys 120:5932
7. Cave RJ, Zhang F, Maitra NT, Burke K (2004) Chem Phys Lett 389:39
8. Huix-Rotllant M, Ipatov A, Rubio A, Casida ME (2011) Chem Phys 391:120
9. Aryasetiawan F, Gunnarsson O, Rubio A (2002) Europhys Lett 57:683
10. McWeeny R (1992) Methods of molecular quantum mechanics. Academic, San Diego
11. Slater JC, Wood JH (1970) Int J Quantum Chem S4:3
12. Ziegler T, Rauk A, Baerends EJ (1977) Theor Chim Acta 43:261
13. Gunnarsson O, Lundqvist BI (1976) Phys Rev B 13:4274
14. Kowalczyk T, Yost SR, Van Voorhis T (2011) J Chem Phys 134:054128
15. Gaudoin R, Burke K (2004) Phys Rev Lett 93:173001
16. Gaudoin R, Burke K (2005) Phys Rev Lett 94:029901
17. Li YQ, Pan XY, Li B, Sahni V (2012) Phys Rev A 85:032517
18. Theophilou AK (1979) J Phys C Solid State Phys 12:5419
19. Valone SM (1980) J Chem Phys 73:4653
20. Lieb EH (1983) Int J Quantum Chem 24:243
21. Englisch H, Englisch R (1984) Phys Stat Sol (b) 123:711
22. Englisch H, Englisch R (1984) Phys Stat Sol (b) 124:373
23. Gross EKU, Oliveira LN, Kohn W (1988) Phys Rev A 37:2805
24. Gross EKU, Oliveira LN, Kohn W (1988) Phys Rev A 37:2809
25. Oliveira LN, Gross EKU, Kohn W (1988) Phys Rev A 37:2821
26. Schipper PRT, Gritsenko OV, Baerends EJ (1998) Theor Chem Acc 99:329
27. Schipper PRT, Gritsenko OV, Baerends EJ (1999) J Chem Phys 111:4056
28. Morrison RC (2002) J Chem Phys 117:10506
29. Oliveira LN, Gross EKU, Kohn W (1990) Int J Quantum Chem Quantum Chem Symp 24:707
30. Ullrich CA, Kohn W (2001) Phys Rev Lett 87:093001
31. Pastorczak E, Gidopoulos NI, Pernal K (2013) Phys Rev A 87:062501
32. Franck O, Fromager E (2014) Mol Phys 112:1684
33. Pribram-Jones A, Yang ZH, Trail JR, Burke K, Needs RJ, Ullrich CA (2014) J Chem Phys 140:18A541
34. Filatov M, Shaik S (1998) Chem Phys Lett 288:689
35. Filatov M, Shaik S (1999) Chem Phys Lett 304:429
36. Filatov M, Shaik S (2000) Chem Phys Lett 332:409
37. Filatov M, Shaik S (2000) J Phys Chem A 104:6628
38. Moreira IDPR, Costa R, Filatov M, Illas F (2007) J Chem Theory Comput 3:764
39. Kazaryan A, Heuver J, Filatov M (2008) J Phys Chem A 112:12980
40. Filatov M (2013) J Chem Theory Comput 9:4526
41. Huix-Rotllant M, Filatov M, Gozem S, Schapiro I, Olivucci M, Ferré N (2013) J Chem Theory Comput 9:3917
42. Filatov M, Shaik S (1999) J Phys Chem A 103:8885
43. Filatov M, Shaik S (1999) J Chem Phys 110:116
44. De Visser SP, Filatov M, Shaik S (2000) Phys Chem Chem Phys 2:5046
45. Filatov M, Shaik S, Woeller M, Grimme S, Peyerimhoff SD (2000) Chem Phys Lett 316:135
46. De Visser SP, Filatov M, Shaik S (2001) Phys Chem Chem Phys 3:1242
47. Kraka E, Anglada J, Hjerpe A, Filatov M, Cremer D (2001) Chem Phys Lett 348:115
48. Cremer D, Filatov M, Polo V, Kraka E, Shaik S (2002) Int J Mol Sci 3:604
49. Gräfenstein J, Kraka E, Filatov M, Cremer D (2002) Int J Mol Sci 3:360
50. Filatov M, Cremer D (2003) Phys Chem Chem Phys 5:2320
51. De Visser SP, Filatov M, Schreiner PR, Shaik S (2003) Eur J Org Chem 21:4199

52. Illas F, Moreira IDPR, Bofill JM, Filatov M (2004) Phys Rev B 70:132414
53. Illas F, Moreira IDPR, Bofill JM, Filatov M (2006) Theor Chem Acc 116:587
54. Kazaryan A, Kistemaker JCM, Schäfer LV, Browne WR, Feringa BL, Filatov M (2010) J Phys Chem A 114:5058
55. Filatov M (2011) ChemPhysChem 12:3348
56. Filatov M (2011) Phys Chem Chem Phys 13:12328
57. Filatov M (2011) Phys Chem Chem Phys 13:144
58. Kazaryan A, Lan Z, Schäfer LV, Thiel W, Filatov M (2011) J Chem Theory Comput 7:2189
59. Filatov M, Huix-Rotllant M (2014) J Chem Phys 141:024112
60. Gozem S, Melaccio F, Valentini A, Filatov M, Huix-Rotllant M, Ferré N, Frutos LM, Angeli C, Krylov AI, Granovsky AA, Lindh R, Olivucci M (2014) J Chem Theory Comput 10:3074
61. Filatov M, Olivucci M (2014) J Org Chem 79:3587
62. Zhao Q, Morrison RC, Parr RG (1994) Phys Rev A 50:2138
63. Sinanoglŭ O (1964) Adv Chem Phys 6:315
64. Giesbertz KJH, Baerends EJ (2010) J Chem Phys 132:194108
65. Kohn W (1986) Phys Rev A 34:737
66. Andrejkovics I, Nagy Á (1998) Chem Phys Lett 296:489
67. Paragi G, Gyémánt IK, Van Doren VE (2000) Chem Phys Lett 324:440
68. Paragi G, Gyémánt IK, Van Doren VE (2001) J Mol Struct Theochem 571:153
69. Noziéres P, Pines D (1966) The theory of quantum liquids. Perseus Books Publishing LLC, Cambridge
70. Becke AD (1988) J Chem Phys 88:1053
71. Wang SG, Schwarz WHE (1996) J Chem Phys 105:4641
72. Csányi G, Arias T (2000) Phys Rev B 61:7348
73. Filatov M (2015) WIREs Comput Mol Sci 5:146
74. Lathiotakis NN, Helbig N, Rubio A, Gidopoulos NI (2014) Phys Rev A 90:032511
75. Fernandez JJ, Kollmar C, Filatov M (2010) Phys Rev A 82:022508
76. Farid B (1998) J Phys Condens Matter 10:L1
77. Hirao K, Nakatsuji H (1973) J Chem Phys 59:1457
78. Hoffmann R, Woodward RB (1965) J Am Chem Soc 87:395
79. Hoffmann R, Woodward RB (1965) J Am Chem Soc 87:2046
80. Woodward RB, Hoffmann R (1969) Angew Chem Int Ed 8:781
81. Vydrov OA, Heyd J, Krukau A, Scuseria GE (2006) J Chem Phys 125:074106
82. Vydrov OA, Scuseria GE (2006) J Chem Phys 125:234109
83. Vydrov OA, Scuseria GE, Perdew JP (2007) J Chem Phys 126:154109
84. Coulson CA, Fischer I (1949) Philos Mag 40:386
85. Kolos W, Wolniewicz L (1965) J Chem Phys 43:2429
86. Van Meer R, Gritsenko OV, Baerends EJ (2014) J Chem Phys 140:024101
87. Schirmer J (1982) Phys Rev A 26:2395
88. Schirmer J, Trofimov AB (1995) J Phys B At Mol Opt Phys 28:2299
89. Trofimov AB, Stelter G, Schirmer J (1999) J Chem Phys 111:9982
90. Trofimov AB, Stelter G, Schirmer J (2002) J Chem Phys 117:6402
91. Schirmer J, Trofimov AB (2004) J Chem Phys 120:11449
92. Silva-Junior MR, Schreiber M, Sauer SPA, Thiel W (2008) J Chem Phys 129:104103
93. Tönshoff C, Bettinger HF (2010) Angew Chem Int Ed 49:4125
94. Plasser F, Pašalić H, Gerzabek MH, Libisch F, Reiter R, Burgdörfer J, Müller T, Shepard R, Lischka H (2013) Angew Chem Int Ed 52:2581
95. Nikiforov A, Gamez JA, Thiel W, Huix-Rotllant M, Filatov M (2014) J Chem Phys 141: 124122
96. Send R, Valsson O, Filippi C (2011) J Chem Theory Comput 7:444
97. Jacquemin D, Zhao Y, Valero R, Adamo C, Ciofini I, Truhlar DG (2012) J Chem Theory Comput 8:1255
98. Moore B II, Autschbach J (2013) J Chem Theory Comput 9:4991

99. Grimme S, Neese F (2007) J Chem Phys 127:154116
100. Zhekova H, Krykunov M, Autschbach J, Ziegler T (2014) J Chem Theory Comput 10:3299
101. Stein T, Kronik L, Baer R (2009) J Am Chem Soc 131:2818
102. Krykunov M, Ziegler T (2013) J Chem Theory Comput 9:2761
103. Dreuw A, Weisman JL, Head-Gordon M (2003) J Chem Phys 119:2943
104. Krykunov M, Seth M, Ziegler T (2014) J Chem Phys 140:18A502
105. Filatov M (2014) J Chem Phys 141:124123
106. Hanazaki I (1972) J Phys Chem 76(14):1982